Opportunistic Interference Alignment for MIMO Interfering Multiple-Access Channels

Hyun Jong Yang, *Member*, *IEEE*, Won-Yong Shin, *Member*, *IEEE*,
Bang Chul Jung, *Member*, *IEEE*, and Arogyaswami Paulraj, *Fellow*, *IEEE*

arXiv:1302.5280v1 [cs.IT] 21 Feb 2013

Abstract

We consider the K-cell multiple-input multiple-output (MIMO) interfering multiple-access channel (IMAC) with time-invariant channel coefficients, where each cell consists of a base station (BS) with M antennas and N users having L antennas each. In this paper, we propose two opportunistic interference alignment (OIA) techniques utilizing multiple transmit antennas at each user: antenna selection-based OIA and singular value decomposition (SVD)-based OIA. Their performance is analyzed in terms of *user scaling law* required to achieve KS degrees-of-freedom (DoF), where $S(\leq M)$ denotes the number of simultaneously transmitting users per cell. We assume that each selected user transmits a single data stream at each time-slot. It is shown that the antenna selection-based OIA does not fundamentally change the user scaling condition if L is fixed, compared with the single-input multiple-output (SIMO) IMAC case, which is given by $\text{SNR}^{(K-1)S}$, where SNR denotes the signal-to-noise ratio. In addition, we show that the SVD-based OIA can greatly reduce the user scaling condition to $\text{SNR}^{(K-1)S-L+1}$ through optimizing a weight vector at each user. Simulation results validate the derived scaling laws of the proposed OIA techniques. The sum-rate performance of the proposed OIA techniques is compared with the conventional techniques in MIMO IMAC channels and it is shown that the proposed OIA techniques outperform the conventional techniques.

Index Terms

Degrees-of-freedom (DoF), opportunistic interference alignment (OIA), MIMO interfering multiple-access channel (MIMO-IMAC), transmit beamforming, user scheduling.

A part of this work was presented in IEEE International Symposium on Information Theory (ISIT), Cambridge, MA, July 2012 [1].

H. J. Yang and A. Paulraj are with the Department of Electrical Engineering, Stanford University, Stanford, CA 94305 (email: hjdbell, apaulraj@stanford.edu).

W.-Y. Shin is with the Division of Mobile Systems Engineering, College of International Studies, Dankook University, Yongin 448-701, Republic of Korea (E-mail: wyshin@dankook.ac.kr).

B. C. Jung (corresponding author) is with the Department of Information and Communication Engineering, Gyeongsang National University, Tongyeong 650-160, Republic of Korea (E-mail: bcjung@gnu.ac.kr).

I. INTRODUCTION

Interference management is a crucial problem in wireless communications. Over the past decade, there has been a great deal of research to characterize the asymptotic capacity inner-bounds of interference channels (ICs) using the simple notion of degrees-of-freedom (DoF), also known as multiplexing gain. Recently, interference alignment (IA) [2]–[10] has emerged as a fundamental solution to achieve the optimal degrees-of-freedom (DoF)[1] in several IC models. The conventional IA technique for the K-user IC [2] and the K-user X channel [9], [10] is based on several strict conditions as follows. Time, frequency, or space domain extension is required to render the channel model multi-dimensional. To this end, channel randomness, i.e., time-varying or frequency-selective channel coefficients, is needed. Moreover, an arbitrarily large size of the dimension extension is needed for K greater than 3, which results in an excessive bandwidth usage is required for the decoding of one signal block [6]. In addition, global channel state information (CSI) is needed at all nodes [2], [3], [8], [11], [12].

For the interfering multiple-access channel (IMAC) consisting of K cells, where each cell is composed of N users and a single base station (BS), Suh and Tse developed a new IA scheme to characterize the DoF achievability of the K-cell IMAC [6] allowing the rank of the interference space to be larger than one. The underlying idea of the IA is to align the interference to the desired interference spaces at the receivers by exploiting diversity (i.e., randomness) in any resource domain. The scheme proposed in [6] utilized the user domain resource for the IA in the IMAC. This IA scheme based on the user diversity leads to two interesting results. First, the DoF of the interference-free network, given by K, can be achieved as N increases. Second, the size of the time/frequency domain extension is greatly reduced. Specifically, the finite size of the extension is given by $O(N)$, which is sufficient to operate for given N. However, arbitrarily large N is needed to attain K DoF, which results in an infinite dimension extension in the end. Thus, time-varying or frequency-selective fading is still required for this scheme.

Recently, the concept of opportunistic interference alignment (OIA) was introduced in [13]–[17], for the K-cell N-user single-input multiple-output (SIMO) IMAC with time-invariant channel coefficients, where each base station (BS) has M antennas. In the OIA technique, opportunistic user scheduling is combined with the spatial domain IA to align the interference to predefined interference spaces at each BS by exploiting multiuser diversity. Although several studies independently addressed some of the aforementioned practical problems of the conventional IA technique [6], [18]–[20], the OIA technique resolved these practical issues simultaneously. The OIA scheme employs the spatial domain IA only with the aid of opportunistic user scheduling and thus operates with a single snapshot without any dimension extension. The purpose of the OIA-related work [13], [15], [16] is not only to maximize the DoF as in the conventional schemes, but also to characterize the trade-off between the achievable DoF and the number of users required. It was shown in [16] that the OIA scheme achieves KS DoF if N scales faster than $\mathrm{SNR}^{(K-1)S}$ in a high SNR regime, where $S(\leq M)$ is the number of selected users in each cell.

In this paper, we introduce an OIA for the K-cell MIMO IMAC with time-invariant channel coefficients, where each cell consists of one BS with M antennas and N users having L antennas each. Inheriting the basic OIA principle [13], the proposed OIA operates with local CSI at the transmitter[2], no inter-user or intercell coordination (i.e., distributed scheduling metric calculation), no dimension extension, and no iterative processing. In [21], the outer bound on the DoF of the MIMO IMAC with time-invariant channel coefficients was characterized, and necessary conditions for M and L needed to achieve the optimal DoF were derived with global CSI at all nodes. However, the main goal of the proposed OIA is to characterize a trade-off between the achievable DoF and the number of users required in the MIMO IMAC with arbitrary M and L. That is, the focus is on studying the user scaling law needed to achieve the target DoF, given by KS, which is optimal if $S = M$. Scaling conditions required to achieve target performance have a great impact in providing the convergence rate to the target performance with respect to considered

[1]The *optimal* DoF denotes the maximum achievable DoF for given channel, which is proved by the converse proof.

[2]In interference channels, the local CSI at the transmitter denotes the information of the channels from the transmitter to all receivers, i.e., its own transmit links [5].

system parameters, thus yielding an intuitive performance measure. For instance, it is common in MIMO systems to evaluate limited feedback schemes by analyzing the relationship between the codebook size scaling and the rate-loss [22], [23], and the concept has been applied also to MIMO ICs [24], [25].

In the downlink cellular IC, user scaling laws were developed for the OIA [21], [26] and for the opportunistic interference management with limited feedback [27], [28]. These schemes cannot be easily extended to the IMAC, because there exists a mismatch between generating interferences at each user and interferences suffered by each BS from multiple users, thus yielding the difficulty of user scheduling design.

More specifically, we propose the following two types of OIA: antenna selection-based OIA and singular value decomposition (SVD)-based OIA. We then derive the scaling law for required N with respect to SNR, under which KS DoF can be achieved. In the proposed schemes, each selected user employs transmit beamforming to mitigate the leakage of interference (LIF) it generates. While the alignment was performed only through user scheduling in the SIMO case, the transmit beamforming is used for the MIMO OIA to perform the spatial domain IA along with opportunistic user scheduling. Moreover, the additional effort for the feedback of the weight vector from each selected user to the corresponding BS is in general required compared to the SIMO case, except for the proposed antenna selection-based OIA.

We show that for the antenna selection-based OIA, where the best transmit antenna is selected at each user, required N scales as $L^{-1}\text{SNR}^{(K-1)S}$. Thus, the user scaling condition with respect to SNR does not fundamentally change, compared with the SIMO IMAC case [16], if L is a constant independent of N. However, the sum-rate gain of the antenna selection-based OIA over the SIMO OIA increases as L grows, whereas no additional feedback is required. For the SVD-based OIA, each user designs the weight vector that minimizes the leakage of interference (LIF) using SVD-based beamforming. We show that the SVD-based OIA can greatly reduce the user scaling condition to $\text{SNR}^{(K-1)S-L+1}$ with the help of the high-rate feedback. Our schemes are compared with the existing IA schemes for multiuser ICs, and computer simulations are provided to validate the derived scaling laws. From this study, besides the fundamental trade-off between the user scaling condition and the achievable DoF, we examine that in the MIMO IMAC, there also exists a trade-off between the amount of feedback for the weight vectors and the user scaling condition.

The organization of this paper is as follows. Section II describes the system and channel models of MIMO IMAC. The proposed the MIMO OIA scheme is presented in Section III. Both DoF achievability analyses and user scaling laws are provided in Section IV. The proposed scheme is compared with the existing MIMO uplink schemes as well as the converse proof in Section V. Section VI provides simulation results and Section VII concludes the paper.

Notations: $\mathbb{C}$ indicates the field of complex numbers. $(\cdot)^T$ and $(\cdot)^H$ denote the transpose and the conjugate transpose, respectively.

II. System and Channel Models

Let us consider the time-division duplex (TDD) K-cell MIMO IMAC, as depicted in Fig. 1. Each cell consists of a BS with M antennas and N users, each with L antennas. The number of users selected to transmit uplink signals in each cell is denoted by $S \leq M$. It is assumed that each selected user transmits a single spatial stream. To consider nontrivial cases, we assume that $L < (K-1)S+1$, because all the inter-cell interference can be completely canceled at the transmitters otherwise[3]. The channel matrix from user j in the i-th cell to BS k (in the k-th cell) is denoted by $\mathbf{H}_k^{[i,j]} \in \mathbb{C}^{M\times L}$, where $i,k \in \mathcal{K} \triangleq \{1,\ldots,K\}$ and $j \in \mathcal{N} \triangleq \{1,\ldots,N\}$. Time-invariant frequency-flat fading is assumed, i.e., channel coefficients are constant during a transmission block, and channel reciprocity between uplink and downlink channels is assumed. From pilot signals sent from all the BSs, user j in the i-th cell can estimate the channels $\mathbf{H}_k^{[i,j]}$, $k = 1,\ldots,K$, utilizing the channel reciprocity, i.e., the local CSI at the transmitter. Without loss of

[3]The case where $L \geq (K-1)S+1$ and where each selected user transmits multiple spatial streams is discussed at the end of Section IV-B (see Remark 3) and also in Section V-B with the comparison to the existing schemes.

generality, the indices of selected users in every cell are assumed to be $(1,\ldots,S)$. The total DoF are defined by

$$\text{DoF} = \lim_{\text{SNR}\to\infty} \frac{\sum_{i=1}^{K}\sum_{j=1}^{S} R^{[i,j]}}{\log \text{SNR}}, \tag{1}$$

where $R^{[i,j]}$ denotes the achievable rate for user j in the i-th cell.

III. Proposed OIA for MIMO IMAC

We first describe the overall procedure of the proposed OIA scheme for MIMO IMAC, and then derive the achievable sum-rate and present the geometric interpretation of the proposed scheme.

A. Overall Procedure

1) Initialization (Reference Basis Broadcast): The interference space for the interference alignment at the k-th cell is denoted by $\mathbf{Q}_k = [\mathbf{q}_{k,1},\ldots,\mathbf{q}_{k,M-S}]$, where $\mathbf{q}_{k,m} \in \mathbb{C}^{M\times 1}$ is the orthonormal basis, $k \in \mathcal{K}$, $m = 1,\ldots,M-S$. BS k independently generates $\mathbf{q}_{k,m}$ from the isotropic distribution over the M-dimensional unit sphere. For given $\mathbf{Q}_k$, BS k also calculates the null space of $\mathbf{Q}_k$, defined by

$$\mathbf{U}_k = [\mathbf{u}_{k,1},\ldots,\mathbf{u}_{k,S}] \triangleq \text{null}(\mathbf{Q}_k), \tag{2}$$

where $\mathbf{u}_{k,i} \in \mathbb{C}^{M\times 1}$ is the orthonormal basis, and broadcasts it to all users prior to the communication. The interference basis $\mathbf{Q}_k$ can be chosen arbitrarily such that $\mathbf{Q}_k$ is full rank. A simple way to maximize the performance of the ZF equalization at the BS, which will be discussed in the sequel, would be choosing $M-S$ columns of the left or right singular matrix of any $M\times M$ matrix as $\mathbf{Q}_k$ and choosing the rest of the S columns as $\mathbf{U}_k$. If $S = M$, then $\mathbf{U}_k$ can be any orthogonal matrix. Note that the calculation and broadcast of $\mathbf{U}_k$ is required only once prior to the communication as $\mathbf{Q}_k$ is determined only by M and S.

2) Stage 1 (Weight Design and Scheduling Metric Feedback): Let us define the unit-norm weight vector at user j in the i-th cell by $\mathbf{w}^{[i,j]}$, i.e., $\left\|\mathbf{w}^{[i,j]}\right\|^2 = 1$. Two different methods to design $\mathbf{w}^{[i,j]}$ shall be presented in Section IV along with the corresponding user scaling law. From the notion of $\mathbf{U}_k$ and $\mathbf{H}_k^{[i,j]}$, user j in the i-th cell calculates its LIF, which is received at BS k and not aligned at the interference space $\mathbf{Q}_k$, from

$$\tilde{\eta}_k^{[i,j]} = \left\|\text{Proj}_{\perp\mathbf{Q}_k}\left(\mathbf{H}_k^{[i,j]}\mathbf{w}^{[i,j]}\right)\right\|^2 \tag{3}$$

$$= \left\|\mathbf{U}_k^H\mathbf{H}_k^{[i,j]}\mathbf{w}^{[i,j]}\right\|^2, \tag{4}$$

where $i \in \mathcal{K}$, $j \in \mathcal{N}$, and $k \in \mathcal{K}\setminus i = \{1,\ldots,i-1,i+1,\ldots,K\}$. The scheduling metric of user j in the i-th cell, denoted by $\eta^{[i,j]}$, is defined by the sum of LIFs, which are not aligned to the interference spaces at neighboring cells. That is,

$$\eta^{[i,j]} = \sum_{k=1,k\neq i}^{K} \tilde{\eta}_k^{[i,j]}. \tag{5}$$

All the users report their LIF metrics to corresponding BSs.

3) Stage 2 (User Selection): Upon receiving N users' scheduling metrics in the serving cell, each BS selects S users having smallest LIF metrics. Note again that we assume without loss of generality that user j, $j = 1,\ldots,S$, in each cell have the smallest LIF metrics and thus are selected. Subsequently, user j in the i-th cell forwards the information on $\mathbf{w}^{[i,j]}$ to BS i for coherent decoding.

4) Stage 3 (Uplink Communication): The transmit signal vector at user j in the i-th cell is given by $\mathbf{w}^{[i,j]}x^{[i,j]}$, where $x^{[i,j]}$ is the transmit symbol with unit average power, and the received signal at BS i can be written as:

$$\mathbf{y}_i = \underbrace{\sum_{j=1}^{S} \mathbf{H}_i^{[i,j]}\mathbf{w}^{[i,j]}x^{[i,j]}}_{\text{desired signal}} + \underbrace{\sum_{k=1,k\neq i}^{K}\sum_{m=1}^{S} \mathbf{H}_i^{[k,m]}\mathbf{w}^{[k,m]}x^{[k,m]}}_{\text{inter-cell interference}} + \mathbf{z}_i, \tag{6}$$

where $\mathbf{z}_i \in \mathbb{C}^{M\times 1}$ denotes the additive noise, each element of which is independent and identically distributed complex Gaussian with zero mean and the variance of SNR^{-1}. As in SIMO IMAC [13], [16], the linear zero-forcing (ZF) detection is applied at the BSs to null inter-user interference for the home cell users' signals. From the notion of $\mathbf{H}_i^{[i,j]}$ and $\mathbf{w}^{[i,j]}$, BS i obtains the sufficient statistics for parallel decoding

$$\mathbf{r}_i = [r_{i,1},\ldots,r_{i,S}]^{\mathrm{T}} \triangleq \mathbf{F}_i{}^H\mathbf{U}_i^H\mathbf{y}_i, \tag{7}$$

where $\mathbf{U}_i$ is multiplied to remove the inter-cell interference components that are aligned at the interference space of BS i, $\mathbf{Q}_i$, and $\mathbf{F}_i \in \mathbb{C}^{S\times S}$ is the ZF equalizer defined by

$$\begin{aligned}\mathbf{F}_i &= [\mathbf{f}_{i,1},\ldots,\mathbf{f}_{i,S}] \\ &\triangleq \left(\left[\mathbf{U}_i{}^H\mathbf{H}_i^{[i,1]}\mathbf{w}^{[i,1]},\ldots,\mathbf{U}_i{}^H\mathbf{H}_i^{[i,S]}\mathbf{w}^{[i,S]}\right]^{-1}\right)^H.\end{aligned} \tag{8}$$

For a comprehensive overview, the overall sequential procedure is illustrated in Fig. 2. Note that we assume low-rate perfect information exchanges for Stages 1–3, such as feedback of the scheduling metric, broadcast of user selection information, feedforward of weight vector information, as in [16], [23]–[26], [29].

B. Sum-Rate Calculation

From (7), the jth spatial stream, $r_{i,j}$, is written as

$$r_{i,j} = x^{[i,j]} + \sum_{k=1,k\neq i}^{K}\sum_{m=1}^{S}\mathbf{f}_{i,j}{}^H\mathbf{U}_i{}^H\mathbf{H}_i^{[k,m]}\mathbf{w}^{[k,m]}x^{[k,m]} + \mathbf{f}_{i,j}{}^H\mathbf{z}_i', \tag{9}$$

where $\mathbf{z}_i' \triangleq \mathbf{U}_i{}^H\mathbf{z}_i$. Thus, $R^{[i,j]}$ is given by

$$\begin{aligned}R^{[i,j]} &= \log\left(1+\text{SINR}^{[i,j]}\right) \\ &= \log\left(1+\frac{\text{SNR}}{\|\mathbf{f}_{i,j}\|^2 + I_{i,j}}\right),\end{aligned} \tag{10}$$

where $\text{SINR}^{[i,j]}$ denotes the signal-to-noise-and-interference ratio of the user j in the i-th cell and $I_{i,j}$ is the sum-interference defined by

$$I_{i,j} = \sum_{k=1,k\neq i}^{K}\sum_{m=1}^{S}\left|\mathbf{f}_{i,j}{}^H\mathbf{U}_i{}^H\mathbf{H}_i^{[k,m]}\mathbf{w}^{[k,m]}\right|^2 \text{SNR}. \tag{11}$$

C. Geometric Interpretation

If $S < M$ and the interference from user m in the k-th cell to BS i is aligned to $\mathbf{Q}_i$, i.e.,

$$\mathbf{H}_i^{[k,m]}\mathbf{w}^{[k,m]} \in \text{span}\left[\mathbf{Q}_i\right], \tag{12}$$

then it is nulled in $\mathbf{r}_i$ because ${\mathbf{U}_i}^H\mathbf{H}_i^{[k,m]}\mathbf{w}^{[k,m]} = \mathbf{0}$, i.e., $\tilde{\eta}_i^{[k,m]} = 0$. If $S = M$, the LIF metric is simplified to $\tilde{\eta}_k^{[i,j]} = \left\|\mathbf{H}_k^{[i,j]}\mathbf{w}^{[i,j]}\right\|^2$. In this case, no IA is conducted and only the opportunistic interference nulling (OIN) is performed as in the OIN for the SIMO IMAC [16]. We do not separately describe this OIN mode, as it can be taken into account by the OIA framework.

Figure 3 illustrates the proposed MIMO OIA for $K = 2$, $M = 3$, and $S = 2$. The interference terms $\mathbf{H}_2^{[1,1]}\mathbf{w}^{[1,1]}$ and $\mathbf{H}_2^{[1,2]}\mathbf{w}^{[1,2]}$ should be aligned to the interference space $\mathbf{q}_{2,1}$ at BS 2, while we only require for the signal vectors $\mathbf{H}_1^{[1,1]}\mathbf{w}^{[1,1]}$ and $\mathbf{H}_1^{[1,2]}\mathbf{w}^{[1,2]}$ to be distinguishable at BS 1. Similarly, $\mathbf{H}_1^{[2,1]}\mathbf{w}^{[2,1]}$ and $\mathbf{H}_1^{[2,2]}\mathbf{w}^{[2,2]}$ should be aligned to $\mathbf{q}_{1,1}$ at BS 1, while $\mathbf{H}_2^{[2,1]}\mathbf{w}^{[2,1]}$ and $\mathbf{H}_2^{[2,2]}\mathbf{w}^{[2,2]}$ need to be distinguishable at BS 2. The main task of the achievability proof is to show that $\tilde{\eta}_k^{[i,j]}$ can be made arbitrarily small for all cross-links through opportunistic scheduling and beamforming, which proves that the IA conditions (12) hold true almost surely for all $i \in \mathcal{K}$, $m \in \mathcal{S} \triangleq \{1, \ldots, S\}$, and $k \in \mathcal{K} \setminus i$. Note that for given $\mathbf{w}^{[i,j]}$, the signal vectors at each BS are distinguishable, since the channel coefficients are generated from continuous distributions. Therefore, in such case, the DoF of KS is achievable.

IV. DoF Achievability

In this section, we present two different beamforming strategies to design $\mathbf{w}^{[i,j]}$ at each user, and characterize the DoF achievability for each strategy in terms of the user scaling law.

A. Antenna Selection

In the antenna selection-based OIA, only one transmit antenna is selected to transmit at each user, i.e., $\mathbf{w}^{[i,j]} \in \{\mathbf{e}_1, \ldots, \mathbf{e}_L\}$, where $\mathbf{e}_l$ denotes the l-th column of the $(L \times L)$-dimensional identity matrix. Let us denote the l-th column of $\mathbf{H}_k^{[i,j]}$ by $\mathbf{h}_{k,l}^{[i,j]}$, $l \in \{1, \ldots, L\}$. Then, user j in the i-th cell chooses the optimal weight vector as $\mathbf{w}_{\text{AS}}^{[i,j]} = \mathbf{e}_{\hat{l}(i,j)}$, where the index $\hat{l}(i,j)$ is obtained from

$$\hat{l}(i,j) = \arg\min_{1 \le l \le L} \sum_{k=1, k\neq i}^{K} \left\|{\mathbf{U}_k}^H\mathbf{h}_{k,l}^{[i,j]}\right\|^2. \tag{13}$$

Then, the corresponding scheduling metric is given by

$$\eta_{\text{AS}}^{[i,j]} = \sum_{k=1, k\neq i}^{K} \left\|{\mathbf{U}_k}^H\mathbf{h}_{k,\hat{l}(i,j)}^{[i,j]}\right\|^2 \tag{14}$$

and is reported to BS i. Since the $\hat{l}(i,j)$-th column of the channel matrix, $\mathbf{h}_{i,\hat{l}(i,j)}^{[i,j]}$, is the effective channel vector at BS i, the feedback is not needed if user j in the i-th cell transmits the uplink pilot to BS i only through the $\hat{l}(i,j)$-th antenna after it is selected to transmit.

The following theorem establishes the DoF achievability of the antenna selection-based OIA.

Theorem 1 (User scaling law: Antenna selection-based OIA): The antenna selection-based OIA with the scheduling metric (14) achieves

$$\text{DoF} \ge KS \tag{15}$$

with high probability if

$$N = \omega\left(L^{-1}\text{SNR}^{(K-1)S}\right), \tag{16}$$

where a function $f(x)$ defined by $f(x) = \omega(g(x))$ implies that $\lim_{x\to\infty} \frac{g(x)}{f(x)} = 0$.

Proof: See Appendix I. ■

Note that in the SIMO IMAC, the OIA scheme achieves the DoF of KS if $N = \omega\left(\text{SNR}^{(K-1)S}\right)$ [16, Theorem 1]. Thus, the antenna selection-based OIA does not fundamentally change the user scaling if L is fixed. Note that however, the user scaling condition is reduced even without any additional feedback, compared to the SIMO case, if L scales with respect to SNR. The following remark discusses the cooperative feature the opportunistic gain obtained from the user and antenna diversity in the antenna selection-based OIA.

Remark 1: If L scales faster than SNR^{ψ_L}, where ψ_L is a positive scalar, then the user scaling condition to achieve the DoF of KS is given by $N = \omega\left(\text{SNR}^{(K-1)S-\psi_L}\right)$. If $\psi_L = (K-1)S$, then the DoF of KS is obtained with high probability for any $N \geq S$. In such case, the opportunistic gain is sufficiently obtained only through the antenna diversity. In other words, the opportunistic gain can be achieved cooperatively from the user and antenna diversity.

Now as a corollary to Theorem 1 in [16], we discuss the upper-bound on the user scaling law with the antenna selection by considering the general case where more than one transmit spatial stream are allowed at each user.

Corollary 1: Suppose that user j in the i-th cell selects $n^{[i,j]}$ transmit antennas with smaller LIF metrics, where the l-th antenna's LIF metric is given by $\sum_{k=1,k\neq i}^{K} \left\|\mathbf{U}_k{}^H \mathbf{h}_{k,l}^{[i,j]}\right\|^2$, $l \in \{1,\ldots,L\}$. Then, the *general antenna selection-based OIA*, in which BS i selects S_i users with smaller sum-LIF metrics, achieves KS DoF with high probability if $N = \omega\left(L^{-1}\text{SNR}^{(K-1)S}\right)$, and if $n^{[i,j]}$ and S_i are chosen such that $S = \sum_{j=1}^{S_i} n^{[i,j]}$, $i \in \mathcal{K}$, and such that the sum-LIF of the selected S spatial channels is minimized at each cell.

Proof: Since the considered scheme is equivalent to selecting S spatial channels (transmit antennas) with smaller LIF metrics amongst NL spatial channels, which is also equivalent to the SIMO OIA with NL users, the proof is immediate from [16, Theorem 1]. ■

Remark 2: In the general antenna selection approach, the optimal $n^{[i,j]}$ should be determined to find the best S spatial channels, which in general requires a joint optimization with global CSI or L times increased the feedback phases for each user to feed back all individual LIF metrics for L antennas. Surprisingly, Theorem 1 indicates that the antenna selection-based OIA with single spatial stream at each user is enough to achieve the same result, in which the scheduling metric is calculated at each user using local CSI without any cooperation or additional feedback. It is more surprising that the selection of the best one out of the L spatial channels at each user does not degrade the diversity gain in terms of the user scaling law, compared to the selection of the best S out of NL spatial channels. The result is encouraging, since we can expect the same benefit of increasing N to NL by simply increasing the number of antennas at the users.

B. SVD-Based OIA

In the SVD-based OIA, each user finds the optimal weight vector that minimizes its LIF metric. The same beamforming technique was also considered in [30], [31] for the MIMO IMAC, however, our focus is to derive a user scaling law and thereby to analytically examine the relationship between the number of users and the beamforming techniques used.

The LIF metric for the SVD-based OIA is defined by

$$\eta_{\text{SVD}}^{[i,j]} = \sum_{k=1,k\neq i}^{K} \left\|\mathbf{U}_k{}^H \mathbf{H}_k^{[i,j]} \mathbf{w}^{[i,j]}\right\|^2 = \left\|\mathbf{G}^{[i,j]} \mathbf{w}^{[i,j]}\right\|^2, \tag{17}$$

where $\mathbf{G}^{[i,j]} \in \mathbb{C}^{(K-1)S\times L}$ is the stacked cross-link channel matrix, defined by

$$\mathbf{G}^{[i,j]} \triangleq \Bigg[\left(\mathbf{U}_1{}^H \mathbf{H}_1^{[i,j]}\right)^T, \ldots, \left(\mathbf{U}_{i-1}{}^H \mathbf{H}_{i-1}^{[i,j]}\right)^T, \left(\mathbf{U}_{i+1}{}^H \mathbf{H}_{i+1}^{[i,j]}\right)^T, \ldots, \left(\mathbf{U}_K{}^H \mathbf{H}_K^{[i,j]}\right)^T \Bigg]^T. \tag{18}$$

Let us denote the SVD of $\mathbf{G}^{[i,j]}$ as

$$\mathbf{G}^{[i,j]} = \mathbf{\Omega}^{[i,j]} \mathbf{\Sigma}^{[i,j]} \mathbf{V}^{[i,j]H}, \tag{19}$$

where $\mathbf{\Omega}^{[i,j]} \in \mathbb{C}^{(K-1)S\times L}$ and $\mathbf{V}^{[i,j]} \in \mathbb{C}^{L\times L}$ consist of L orthonormal columns, and $\mathbf{\Sigma}^{[i,j]} = \text{diag}\left(\sigma_1^{[i,j]}, \ldots, \sigma_L^{[i,j]}\right)$, where $\sigma_1^{[i,j]} \geq \cdots \geq \sigma_L^{[i,j]}$. Then, it is apparent that the optimal $\mathbf{w}^{[i,j]}$ is determined as

$$\mathbf{w}_{\text{SVD}}^{[i,j]} = \arg\min_{\mathbf{v}} \left\|\mathbf{G}^{[i,j]}\mathbf{v}\right\|^2 = \mathbf{v}_L^{[i,j]}, \tag{20}$$

where $\mathbf{v}_L^{[i,j]}$ is the L-th column of $\mathbf{V}^{[i,j]}$. With this choice the LIF metric is simplified to

$$\eta_{\text{SVD}}^{[i,j]} = {\sigma_L^{[i,j]}}^2. \tag{21}$$

All the users report their LIF metrics to the corresponding BSs and BS i selects S users with smaller $\eta_{\text{SVD}}^{[i,j]}$ values among N users than the rest. To construct $\mathbf{F}_i$ defined in (8) at BS i for given selected user j, $i = 1, \ldots, K$, $j = 1, \ldots, S$, the information of $\mathbf{w}_{\text{SVD}}^{[i,j]}$ needs to be known by BS i through the feedback with a sufficiently high rate.

At this point, we introduce a useful lemma for the polynomial expression of the CDF of $\eta_{\text{SVD}}^{[i,j]}$.

Lemma 1 (CDF of $\eta_{SVD}^{[i,j]}$): The CDF of $\eta_{\text{SVD}}^{[i,j]}$, denoted by $F_\sigma(x)$, can be written as

$$F_\sigma(x) = \alpha x^{(K-1)S-L+1} + o\left(x^{(K-1)S-L+1}\right), \tag{22}$$

for $0 \leq x < 1$, where α is a constant determined by K, S, and L.

Proof: See Appendix II. ■

Now the following theorem establishes the DoF achievability of the SVD-based OIA.

Theorem 2 (User scaling law: SVD-based OIA): The proposed SVD-based OIA scheme with the scheduling metric (21) achieves

$$\text{DoF} \geq KS \tag{23}$$

with high probability if

$$N = \omega\left(\text{SNR}^{(K-1)S-L+1}\right). \tag{24}$$

Proof: See Appendix III. ■

Therefore, unlike the antenna selection, the SVD-based OIA fundamentally lowers the power of the SNR scaling condition required to achieve the DoF of KS. Note that however, this reduced scaling is achieved at the cost of the sufficiently high-rate feedback of $\mathbf{w}_{\text{SVD}}^{[i,j]}$ from all the selected users to associated BSs. Noting that the antenna selection-based OIA needs no feedback, the antenna selection- and SVD-based OIA schemes are the two extremes of the trade-off between the feedback amount and the user scaling condition to achieve the DoF of KS.

The following remark discusses the trivial case of the SVD-based OIA in terms of the antenna configuration, where the inter-cell interference is perfectly canceled only through transmit beamforming.

Remark 3: Note that if $L \geq (K-1)S + 1$, then $\mathbf{G}^{[i,j]} \in \mathbb{C}^{(K-1)S\times L}$ in (18) becomes a wide matrix and the singular value corresponding to $\mathbf{v}_L^{[i,j]}$ is 0. Therefore, $\mathbf{w}^{[i,j]}$ can be chosen such that $\eta_{\text{SVD}}^{[i,j]} = 0$. The result is intuitively immediate because the total rank of the effective interfering channels from each user to neighboring cells is $(K-1)S$ and because at least one additional rank is required for each user

to transmit one data stream. From this result, it can be easily seen that in the case where each selected user transmits $a \leq M$ data streams, all the inter-cell interference will be canceled through the SVD-based OIA if $L \geq (K-1)Sa + a$. In such case, the number of selected users, S, should be equal to or lower than $\lfloor \frac{M}{a} \rfloor$.

C. User Scaling Laws for Cell-Dependent L, M, N, and S

In this subsection, we examine the user scaling laws for the case where L, M, N, and S are different from cells. Let us denote these parameters at the i-th cell by L_i, M_i, N_i, and S_i, respectively. The following theorem establishes the user scaling laws under this scenario.

Theorem 3: With the cell-dependent parameters, the antenna selection- and SVD-based OIA schemes achieve KS DoF with high probability if

$$N_i = \omega\left(\text{SNR}^{S_i' K}\right), \text{ and } N_i = \omega\left(\text{SNR}^{S_i' K - L_i + 1}\right), \tag{25}$$

respectively, where $S_i' = \sum_{k \neq i, k=1}^{K} S_k$.

Proof: See Appendix IV. ■

From Theorem 3, it is seen that growing the number of serving users at the i-th cell, S_i, increases the number of users required at all other cells for both the antenna selection- and SVD-based OIA. This is because increasing S_i implies a reduced rank of the interference space at the i-th cell, on which users from the other cells attempt to align their signals. For the SVD-based OIA, large L_i reduces the user scaling condition of only the i-th cell.

V. Comparison with Upper Bounds and Existing Schemes

In this section, to verify the optimality of the proposed OIA schemes, we introduce an upper bound on the DoF. We also compare our schemes with existing schemes in terms of the achievable DoF and the computational complexity.

A. Upper Bounds for DoF

We now show an upper limit on the DoF in MIMO IMAC and discuss how to achieve the DoF upper bound. For completeness, we briefly review Corollary 1 of [21] in which the outer bound on the DoF of the MIMO IMAC is given by

$$\text{DoF} \leq \min\left\{NKL, KM, \frac{NK\max\left(NL, (K-1)M\right)}{N+K-1}, \frac{NK\max\left((K-1)L, M\right)}{N+M-1}\right\}. \tag{26}$$

Now it is shown that choosing $S = M$, the proposed schemes achieve KM DoF with arbitrarily large N scaling according to (16) and (24). Note again that with this choice, interference nulling is carried out through opportunistic user scheduling. As N increases, the outer bound (26) is reduced to KM, and hence, our schemes can asymptotically achieve the optimal DoF.

B. DoF Comparison with Existing Methods

In this subsection, the proposed OIA schemes are compared with the two existing strategies [8], [21] that also achieve the optimal DoF in K-cell MIMO uplink networks. Let us first consider the K-user MIMO IC [8] with time-invariant or frequency-selective fading, which can be regarded as a MIMO IMAC with $N = 1$. Consider the case where $L > M$. Then both the scheme in [8] and the proposed SVD-based OIA with each user transmitting M spatial streams achieve the optimal DoF, given by KM, if $L \geq KM$ [8, Theorem 3]. Note that in this case, interference can be perfectly nulled only through

SVD-based beamforming and thus no opportunistic gain is needed (refer to Remark 3). The achievable scheme in [8] operates under time-varying or frequency selective fading channels with global CSI at all nodes, and the size of the time/frequency domain extension is given by $(L/M+1)(n+1)^{\Gamma}$, where $\Gamma = KL/M \cdot (K - L/M - 1)$ and n should be arbitrarily large to obtain KM DoF. For the K-user MIMO IC with time-invariant channel coefficients [8], a necessary condition for the parameter M is also needed to achieve the optimal DoF, which is given by $M \leq (K-2)L$ for $K > 4$. Hence, arbitrarily large M is also required as K increases, whereas our schemes have no necessary condition for M.

Now, let us turn to the K-cell MIMO IMAC studied in [21]. For $K = 2$, both the transmit zero forcing scheme in [21] and the proposed SVD-based OIA with $N = M$ achieves the $2M$ DoF if $L \geq (K-1)M+1 = M+1$. However, for $K > 2$, the scheme in [21] needs the necessary condition $M \geq KS$ to obtain KS DoF [21, Theorem 3], which is not needed in the proposed OIA schemes. Moreover, the precoding matrices are designed based on the notion of global CSI in [21].

C. Computational Complexity

In this subsection, we briefly discuss the computational complexity of the two proposed schemes and compare it to the complexity of the SISO IMAC scheme, Suh and Tse's scheme. The computational effort is analyzed in two-fold: the user computation and the BS computation. We omit the analysis of the detection and decoding complexity after the equalization at each BS, since it is all the same for the schemes considered.

1) Antenna selection-based OIA: Each user calculates (13), from which the scheduling metric (14) can also be obtained. From the results of [32], [33], it can be easily shown that the calculation of (13) requires $8(K-1)MLS + 6(K-1)LS - 2L$ floating point operations (flops), real additions or multiplications; thus, the complexity can be denoted by $O(KLMS)$.

Upon receiving N scheduling metrics, each BS selects S users with smaller scheduling metrics out of N users, which can be performed with linear-time complexity, i.e., $O(N)$, by the partial sorting algorithm [34]. Next, the construction of the effective channel matrix, i.e., ${\mathbf{F}_i}^{-H}$ (See (8)), requires $8MS^2 - 2S^2$ flops. The inversion of this effective channel matrix to get $\mathbf{F}_i$ needs $O(S^3)$ flops, and the calculation of $\mathbf{r}_i$ given in (7) requires $8MS + 8S^2 - 4S$ flops. Therefore, noting that $S \leq M$, the overall computational complexity at each BS is $O(N + MS^2)$.

2) SVD-based OIA: Each user first constructs $\mathbf{G}^{[i,j]}$ defined in (18), which requires $8(K-1)MLS - 2(K-1)LS$ flops, i.e., $O(KLMS)$. Note that the weight vector and the scheduling metric can be simultaneously obtained from the SVD of $\mathbf{G}^{[i,j]}$. The efficient and precise SVD method based on the Householder reflections and the QR decomposition can be performed with $O\left(KSL^2\right)$ flops [35]. Consequently, the computational complexity of the SVD-based OIA at each user is $O(KSL^2 + KLMS)$.

All the procedure at each BS is the same as that of the antenna selection-based OIA except the construction of the effective channel matrix, which requires $8MLS + 8MS^2 - 2MS - 2S^2$ flops. Consequently, the overall complexity at each BS is given by $O(N + MLS + MS^2)$.

Table I summarizes the computational complexity of the OIA schemes with the comparison to the SIMO case. It is obvious that the complexity is the lowest for the SIMO OIA and is the highest for the SVD-based OIA. It is seen that as L increases, the complexity difference between the three schemes becomes greater.

3) SISO IMAC: Now we briefly discuss the computational complexity of Suh and Tse's scheme [6]. Since this scheme applies only to the SISO IMAC, the comparison to this scheme is to roughly show the computational efficiency of the proposed schemes. Each user in Suh and Tse's scheme finds the inversions of $K-1$ $(n \times n)$-dimensional matrices and the Kronecker multiplications of $K-1$ n-dimensional vectors, where $n = \sqrt[K-1]{N} + 1$. This calculation at each user requires $O(N + K\sqrt[K-1]{N}^3)$ flops. Another heavy calculation in this scheme is to find the $(K-1)$-level decompositions of $n^{K-1} \times n^{K-1}$ matrices, which cannot be systematically performed. In addition, the complexity for the equalization at each BS is dominated by the effort to find the inversion of an $(n^{K-1} \times n^{K-1})$-dimensional matrix, which needs $O(N^3)$ flops.

Considering the fact that Suh and Tse's scheme requires much lower dimension extension size than the conventional IA schemes and thus is already computationally attractive, the proposed schemes is more computationally effective compared to the previous schemes. In addition, it should be stressed that both the dimension extension size and N need to be arbitrarily large to achieve the optimal DoF with Suh and Tse's scheme, whilst arbitrarily large N suffices the condition for the optimal DoF for the proposed schemes.

VI. Simulation Results

In this section, through computer simulations, we evaluate the sum of LIF and the sum-rate of the proposed OIA schemes, operating with finite N and SNR in the MIMO IMAC. The max-SNR scheme is compared, in which the weight vectors and the scheduling metrics are calculated at each user in a distributed manner only with local CSI. Specifically, each user employs eigen-beamforming to maximize its effective SNR and each BS selects S users having higher effective SNRs up to the S-th largest one. The OIA scheme employing a fixed weight vector, i.e., $\mathbf{w}^{[i,j]} = \mathbf{e}_1$ for all users, is also considered, which can be treated as the OIA scheme for SIMO IMAC. Thus, we refer this scheme as 'SIMO OIA'.

Figure **??** depicts the log-log plot of the sum of LIF, termed as sum-LIF, i.e., $\sum_{i=1}^{K}\sum_{j=1}^{S}\eta^{[i,j]}$, versus N when $K = 3$, $M = L = 2$, and SNR is 10dB. This performance measurement enables us to measure the quality of the proposed OIA schemes, as shown in [5]. Specifically, Fig. **??** exhibits how rapidly the network becomes an error-free network with respect to N. Since the user selection of the max-SNR scheme does not contribute to the reduction of the LIF, the sum-LIF of the max-SNR scheme remains constant for increasing N. The sum-LIF of the antenna selection-based OIA decreases with respect to N at the same rate of the SIMO OIA, because the antenna selection-based OIA is subject to the user scaling condition $\mathrm{SNR}^{(K-1)S}$ if L is fixed. On the other hand, the decreasing rate of the SVD-based OIA is higher, which is subject to the user scaling condition $\mathrm{SNR}^{(K-1)S-L+1}$. As S decreases, the decreasing rates of both the antenna selection- and SVD-based OIA schemes become higher due to the lowered scaling conditions.

Figure **??** shows the log-log plot of the sum-LIF versus L when $K = 3$, $M = 3$, and $N = 100$. For the antenna selection-based OIA, the sum-LIF decreases linearly in log-log scale. On the other hand, the sum-LIF of the SVD-based OIA decreases much faster than the antenna selection-based OIA case and becomes zero if $L \geq (K-1)S+1 = 5$ (refer to Remark 3). Note that however, the feedback redundancy for the weight vectors grows as L increases in the SVD-based OIA, whereas no feedback is required regardless of L in the antenna selection-based OIA.

Figure 6 depicts the sum-rates versus SNR when $K = 3$, and $M = L = 2$ for (a) $N = 20$ and (b) $N = 100$. The sum-rates of the considered schemes are saturated in the sufficiently high SNR regime, because the inter-cell interference cannot approach zero for fixed N values. That is, the SINR will be upper-bounded by a finite value for all schemes. In fact, S determines the amount of the interference level as well as the total DoF. For the max-SNR scheme, the interference at each BS increases as S increases, whereas the sum-rate is increased by S times. The rate at each BS is approximately given by $S\log\left(1+\frac{\mathrm{SNR}}{1+(K-1)S\cdot\Delta}\right)$, where Δ denotes the amount of the interference received from a single user in a neighboring cell. Since this rate is a monotonically increasing function of S, the rate of the max-SNR scheme grows with S. On the other hand, the proposed schemes can significantly suppress the interference. Hence, the cases with $S = 2$ show higher sum-rates than the cases with $S = 1$ in the low SNR regime where the noise is dominant over the interference, and vice versa in the high SNR regime where it becomes more important to minimize the interference. As N increases, the interference can be more reduced, and thus the crossover SNR points, where the sum-rates for the cases $S = 1$ and $S = 2$ are identical, become higher. From Fig. 6, the crossover SNR points of the antenna selection-based OIA appear approximately at 6dB when $N = 20$ and at 9.1dB when $N = 100$, whereas those of the SVD-based OIA are 8.1dB when $N = 20$ and 12.1dB when $N = 100$.

Figure 7 depicts the sum-rates versus N when $K = 3$, $M = L = 2$, and SNR is 20dB. For each of the scheme, the best S value was applied accordingly, which shows higher achievable rates. It is apparent that for infinitely large N, the rates of all the OIA schemes will be the same as those of the interference-free network. It can be seen from the figure that the SVD-based OIA with $S = 1$ approaches the upper-bound most rapidly, since the interference can be made smaller than that of the other OIA schemes according to the given scaling laws. While the SIMO OIA is inferior to the max-SNR scheme if $N \leq 20$, both the proposed OIA schemes exhibit higher sum-rates than those of the max-SNR scheme if $N > 3$.

Finally, Fig. 8 illustrates the symbol error rate (SER) averaged over all users versus N when $K = 3$, $M = L = 2$, $S = 1$, and SNR is 20dB. The block length for each channel instance was assumed to be 50 symbols and quadrature phase shift keying (QPSK) modulation was used. For comparison, we considered the intercell interference-free scheme with the random user selection, which is labeled as 'Interference-Free' in the figure. It is shown that the SERs of all the OIA schemes approach to the SER of the interference-free scheme as N increases. The trends for the approaching rates comply with the results of Theorem 1 and 2; that is, a lower user scaling condition implies better performance, a higher approaching rate in this case.

VII. Conclusion

We have proposed two OIA schemes for the MIMO IMAC and have derived the user scaling law required to achieve the target KS DoF. Although the antenna selection-based OIA cannot fundamentally change the user scaling law compared to the SIMO case, it can increase the achievable rate even with fixed L and with no feedback. Moreover, if L scales also with respect to SNR, then the scaling condition is linearly reduced with respect to L. It was also shown that the user scaling condition can be significantly reduced to $\text{SNR}^{(K-1)-L+1}$ using the SVD-based OIA with help of optimizing a beamforming vector at each user. Furthermore, the achievable rate of the proposed OIA techniques outperform the conventional user scheduling schemes including SIMO OIA.

From this study on the user scaling law, we characterized the lower- and upper-bounds for the trade-off between the number of users required to achieve a target DoF and the amount of the feedback for the weight vectors. Even with the practical rages of the parameters, the user scaling law is a powerful tool to analytically compare the performance, such as the achievable rates or DoF, of any OIA schemes for given number of users.

It can be conjectured that the MIMO OIA with limited feedback for the weight vectors will make a bridge between the proposed two OIA schemes. As our future work, the scaling law for the number of users as well as the feedback size will be studied.

Appendix I
Proof of Theorem 1

From (10) and (11), $\text{SINR}^{[i,j]}$ can be written as

$$\text{SINR}^{[i,j]} = \frac{\text{SNR}}{\|\mathbf{f}_{i,j}\|^2 + I_{i,j}} \tag{27}$$

$$\geq \frac{\text{SNR}/\|\mathbf{f}_{i,j}\|^2}{1 + \sum_{k=1,k\neq i}^{K} \sum_{m=1}^{S} \left\| \mathbf{U}_i{}^H \mathbf{h}_{i,\hat{l}(k,m)}^{[k,m]} \right\|^2 \text{SNR}}. \tag{28}$$

It is apparent that the DoF of KS is achieved if the interference term in the denominator of the right-hand side of (28) remains constant for increasing SNR. At this point, let us define $\mathcal{P}_{\text{AS}}$ by

$$\mathcal{P}_{\text{AS}} \triangleq \lim_{\text{SNR}\to\infty} \Pr\Bigg\{ \sum_{k=1,k\neq i}^{K} \sum_{m=1}^{S} \left\| \mathbf{U}^H \mathbf{h}_{i,\hat{l}(k,m)}^{[k,m]} \right\|^2 \text{SNR} \leq \epsilon, \\ \forall \text{ user } j \text{ in the } i\text{-th cell}, i \in \mathcal{K}, j \in \mathcal{S} \Bigg\}, \tag{29}$$

where $\epsilon > 0$ is a positive constant. Then, DoF is bounded as

$$\text{DoF} \geq KS \cdot \mathcal{P}_{\text{AS}}. \tag{30}$$

When calculating the lower bound (30), we assumed that the DoF of KS is achieved if the interference remains constant for increasing SNR, and zero DoF is achieved otherwise.

The essential of the OIA is the fact that the sum of the received interference terms is equivalent to the sum of the LIF metrics of the selected users. That is,

$$\sum_{i=1}^{K} \sum_{k=1,k\neq i}^{K} \sum_{m=1}^{S} \left\| \mathbf{U}_i{}^H \mathbf{h}_{i,\hat{l}(k,m)}^{[k,m]} \right\|^2 = \sum_{i=1}^{K} \sum_{j'=1}^{S} \eta_{\text{AS}}^{[i,j']}. \tag{31}$$

Subsequently, defining

$$\tilde{I}_{\text{AS},i} \triangleq \sum_{k=1,k\neq i}^{K} \sum_{m=1}^{S} \left\| \mathbf{U}_i{}^H \mathbf{h}_{i,\hat{l}(k,m)}^{[k,m]} \right\|^2, \tag{32}$$

we find the following lower-bound of $\mathcal{P}_{\text{AS}}$:

$$\mathcal{P}_{\text{AS}} \geq \lim_{\text{SNR}\to\infty} \Pr\left\{ \sum_{i=1}^{K} \sum_{j=1}^{S} \tilde{I}_{\text{AS},i} \text{SNR} \leq \epsilon \right\} \tag{33}$$

$$= \lim_{\text{SNR}\to\infty} \Pr\left\{ \sum_{j=1}^{S} \sum_{i=1}^{K} \sum_{j'=1}^{S} \eta_{\text{AS}}^{[i,j']} \text{SNR} \leq \epsilon \right\} \tag{34}$$

$$\geq \underbrace{\lim_{\text{SNR}\to\infty} \Pr\left\{ \eta_{\text{AS}}^{[i,j']} \leq \frac{\text{SNR}^{-1}\epsilon}{KS^2}, \forall i \in \mathcal{K}, \forall j' \in \mathcal{S} \right\}}_{\triangleq \mathcal{P}_{\text{AS}}^0}, \tag{35}$$

where (34) follows from (31). Unlike in the SIMO case [16, Theorem 1], $\eta_{\text{AS}}^{[i,j]}$ is the minimum of L independent Chi-square random variables with degrees-of-freedom of $2(K-1)S$, $\left\| \mathbf{U}_i{}^H \mathbf{h}_{i,l}^{[k,m]} \right\|^2$, $l = 1, \ldots, L$. We denote the probability that user j in the i-th cell has at least one transmit antenna with the scheduling metric lower than $\frac{\epsilon \text{SNR}^{-1}}{KS^2}$ as

$$P_a \triangleq 1 - \Pr\Bigg\{ \sum_{k=1,k\neq i}^{K} \left\| \mathbf{U}_k{}^H \mathbf{h}_{k,l}^{[i,j]} \right\|^2 > \frac{\epsilon \text{SNR}^{-1}}{KS^2}, \\ \forall l \in \{1, \ldots, L\} \Bigg\}. \tag{36}$$

It can be easily verified that P_a is identical and independent for all users. Let us denote the right-hand side of (35) by $\mathcal{P}_{\text{AS}}^0$. Note that $\mathcal{P}_{\text{AS}}^0$ represents the probability that there exist at least S users in each cell,

which have the scheduling metrics lower than $\frac{\epsilon \text{SNR}^{-1}}{KS^2}$, and thus we have

$$\mathcal{P}_{\text{AS}}^0 = 1 - \lim_{\text{SNR}\to\infty} \sum_{i=0}^{S-1} \binom{N}{i} {P_a}^i \cdot (1-P_a)^{N-i}. \tag{37}$$

Denoting by $F(x)$ the cumulative density function (CDF) of a chi-square random variable with the degrees-of-freedom of $2(K-1)S$, we have

$$P_a = 1 - \left(1 - F\left(\frac{\epsilon \text{SNR}^{-1}}{KS^2}\right)\right)^L. \tag{38}$$

Applying (38) to (37), we get (39) and (40) at the bottom of the next page, where C_1 and C_2 are constants independent of SNR and L, defined by

$$C_1 = \frac{e^{-1}2^{-(K-1)S}}{(K-1)S \cdot \Gamma((K-1)S)} \cdot \left(\frac{\epsilon}{KS^2}\right)^{(K-1)S}, \tag{41}$$

$$C_2 = \frac{2^{-(K-1)S+1}}{(K-1)S \cdot \Gamma((K-1)S)} \cdot \left(\frac{\epsilon}{KS^2}\right)^{(K-1)S}. \tag{42}$$

Here, (40) follows from the fact that [15, Lemma 1]

$$\frac{e^{-1}2^{-(K-1)S}}{(K-1)S \cdot \Gamma((K-1)S)} \cdot x^{-(K-1)S} \le F(x), \tag{43}$$

$$F(x) \le \frac{2^{-(K-1)S+1}}{(K-1)S \cdot \Gamma((K-1)S)} \cdot x^{-(K-1)S} \tag{44}$$

and from the fact that $\frac{N!}{i!(N-i)!} \le N^i$. Here, if we choose ϵ small enough such that $C_2\text{SNR}^{-(K-1)S} < 1/L$ for given SNR, we get

$$\left(1 - C_2\text{SNR}^{-(K-1)S}\right)^L > 1 - LC_2\text{SNR}^{-(K-1)S}, \tag{45}$$

which follows from the fact that $1 - xy < (1-x)^y$ for any $0 < x < 1 < y$ and $xy \le 1$. Now, inserting (45) to (40) gives us

$$\mathcal{P}_{\text{AS}}^0 \ge 1 - \lim_{\text{SNR}\to\infty} \sum_{i=0}^{S-1} \frac{\left(NLC_2\text{SNR}^{\delta}\right)^i \left(1 - C_1\text{SNR}^{\delta}\right)^{LN}}{\left(1 - C_2\text{SNR}^{\delta}\right)^{Li}}, \tag{46}$$

where $\delta = -(K-1)S$. If $LN = \omega\left(\text{SNR}^{(K-1)S}\right)$, then $\left(1 - C_1\text{SNR}^{-(K-1)S}\right)^{LN}$ decreases exponentially with respect to SNR, whereas $\left(NLC_2\text{SNR}^{-(K-1)S}\right)^i$ increases polynomially for any $i > 0$. Therefore, $\mathcal{P}_{\text{AS}}^0$ tends to 1 as SNR goes to infinity, and thereby $\mathcal{P}_{\text{AS}}$ tends to 1. This proves the theorem together with (30).

$$\mathcal{P}_{\text{AS}}^0 = 1 - \lim_{\text{SNR}\to\infty} \sum_{i=0}^{S-1} \frac{N!}{i!(N-i)!} \frac{\left(1 - \left(1 - F\left(\frac{\epsilon \text{SNR}^{-1}}{KS^2}\right)\right)^L\right)^i \left(1 - F\left(\frac{\epsilon \text{SNR}^{-1}}{KS^2}\right)\right)^{LN}}{\left(1 - F\left(\frac{\epsilon \text{SNR}^{-1}}{KS^2}\right)\right)^{Li}} \tag{39}$$

$$\ge 1 - \lim_{\text{SNR}\to\infty} \sum_{i=0}^{S-1} \frac{\left\{N\left(1 - \left(1 - C_2 \cdot \text{SNR}^{-(K-1)S}\right)^L\right)\right\}^i \left(1 - C_1\text{SNR}^{-(K-1)S}\right)^{LN}}{\left(1 - C_2\text{SNR}^{-(K-1)S}\right)^{Li}}, \tag{40}$$

APPENDIX II
PROOF OF LEMMA 1

Since $\mathbf{U}_k$ is chosen from an independent isotropic distribution and $\mathbf{H}_k^{[i,j]}$ is an i.i.d. complex Gaussian random matrix, for all $i,k \in \mathcal{K}$, $j \in \mathcal{S}$, $\mathbf{G}^{[i,j]}$ is also an i.i.d. complex Gaussian random matrix. Furthermore, both of $\mathbf{U}_k$ and $\mathbf{H}_k^{[i,j]}$ are chosen from the continuous distributions, and thus have full ranks almost surely [36]. The LIF metric $\eta_{\text{SVD}}^{[i,j]} = {\sigma_L^{[i,j]}}^2$ is the smallest eigen value of the $(L \times L)$-dimensional central Wishart matrix ${\mathbf{G}^{[i,j]}}^H \mathbf{G}^{[i,j]}$. Therefore, from [37, Theorem 4], the polynomial CDF of the smallest eigen value of the full-rank Wishart matrix which is constructed from a $((K-1)S \times L)$-dimensional complex Gaussian matrix has the smallest power of $(K-1)S-L+1$ with the multiplicative coefficient α defined by

$$\alpha \triangleq \frac{\Gamma_{L-1}(1)}{((K-1)S-L+1)!\Gamma_L(L)} \left|\mathbf{\Xi}\right|. \tag{47}$$

Here, $\Gamma_s(t)$ is the normalized complex multivariate gamma function, i.e., $\Gamma_s(t) = \prod_{i=1}^{s}(t-i)!$, and $\mathbf{\Xi}$ is an $(L \times L)$-dimensional integer matrix defined as

$$\{\mathbf{\Xi}\}_{i,j} = \begin{cases} \begin{pmatrix} L-i \\ j-i \end{pmatrix} & i = 1,\ldots,L-1, j = 1,\ldots,L, \\ & j \geq i \\ \frac{(-1)^{i-j}(L-j)!}{(n-j)!} & i = 1,\ldots,L, j = 1,\ldots,L, j \leq i \\ 0 & \text{otherwise}. \end{cases} \tag{48}$$

Therefore, α is determined only by K, S, and L, which proves the lemma.

APPENDIX III
PROOF OF THEOREM 2

From the $\text{SINR}^{[i,j]}$ lower bound, given by

$$\text{SINR}^{[i,j]} \geq \frac{\text{SNR}/\left\|\mathbf{f}_{i,j}\right\|^2}{1+\sum_{k=1,k\neq i}^{K}\sum_{m=1}^{S}\left\|{\mathbf{U}_i}^H \mathbf{H}_i^{[k,m]} \mathbf{w}_{\text{SVD}}^{[k,m]}\right\|^2 \text{SNR}}, \tag{49}$$

we again consider the lower bound of the DoF as

$$\text{DoF} \geq KS \cdot \mathcal{P}_{\text{SVD}}, \tag{50}$$

$$\mathcal{P}_{\text{SVD}} \triangleq \lim_{\text{SNR}\to\infty} \Pr\Bigg\{ \tilde{I}_{\text{SVD},i}\text{SNR} \leq \epsilon, \\ \forall \text{ user } j \text{ in the } i\text{-th cell}, i \in \mathcal{K}, j \in \mathcal{S} \Bigg\}, \tag{51}$$

where

$$\tilde{I}_{\text{SVD},i} = \sum_{k=1,k\neq i}^{K}\sum_{m=1}^{S}\left\|{\mathbf{U}_i}^H \mathbf{H}_i^{[k,m]} \mathbf{w}_{\text{SVD}}^{[k,m]}\right\|^2. \tag{52}$$

Similarly to (31) to (35), the lower bound on $\mathcal{P}_{\text{SVD}}$ is obtained from

$$\mathcal{P}_{\text{SVD}} \geq \lim_{\text{SNR}\to\infty} \Pr\left\{ \sum_{i=1}^{K}\sum_{j=1}^{S} \tilde{I}_{\text{SVD},i}\text{SNR} \leq \epsilon \right\} \tag{53}$$

$$= \lim_{\text{SNR}\to\infty} \Pr\left\{ \sum_{j=1}^{S}\sum_{i=1}^{K}\sum_{j'=1}^{S} \eta_{\text{SVD}}^{[i,j']}\text{SNR} \leq \epsilon \right\} \tag{54}$$

$$\geq \lim_{\text{SNR}\to\infty} \Pr\left\{ \eta_{\text{SVD}}^{[i,j']} \leq \frac{\text{SNR}^{-1}\epsilon}{KS^2}, \forall i \in \mathcal{K}, \forall j' \in \mathcal{S} \right\} \tag{55}$$

The right-hand side of (55) is the probability that there exist at least S users with the scheduling metrics lower than $\frac{\mathrm{SNR}^{-1}\epsilon}{KS^2}$. Noting that the scheduling metrics $\eta_{\mathrm{SVD}}^{[i,j]}$, $i=1,\ldots,K$, $j=1,\ldots,S$, are identically distributed, the right-hand side of (55), denoted by $\mathcal{P}_{\mathrm{SVD}}^0$, can be expressed as

$$\mathcal{P}_{\mathrm{SVD}}^0 = 1 - \lim_{\mathrm{SNR}\to\infty} \sum_{i=0}^{S-1} \binom{N}{i} \left(F_\sigma\left(\frac{\epsilon \mathrm{SNR}^{-1}}{KS^2}\right)\right)^i \times \left(1 - F_\sigma\left(\frac{\epsilon \mathrm{SNR}^{-1}}{KS^2}\right)\right)^{N-i} \tag{56}$$

Denoting $\rho \triangleq (K-1)S + L - 1$, we further have

$$\begin{aligned}\mathcal{P}_{\mathrm{SVD}}^0 &= 1 - \lim_{\mathrm{SNR}\to\infty} \sum_{i=0}^{S-1} \frac{N!}{i!(N-i)!} \\ &\quad \times \frac{\left(\Psi \mathrm{SNR}^{-\rho} + o\left(\mathrm{SNR}^{-\rho}\right)\right)^i}{\left(1 - \Psi \mathrm{SNR}^{-\rho} - o\left(\mathrm{SNR}^{-\rho}\right)\right)^i} \\ &\quad \times \left(1 - \Psi \mathrm{SNR}^{-\rho} - o\left(\mathrm{SNR}^{-\rho}\right)\right)^N \qquad (57) \\ &\geq 1 - \lim_{\mathrm{SNR}\to\infty} \sum_{i=0}^{S-1} \frac{\left\{N\left(\Psi \mathrm{SNR}^{-\rho} + o\left(\mathrm{SNR}^{-\rho}\right)\right)\right\}^i}{\left(1 - \Psi \mathrm{SNR}^{-\rho} - o\left(\mathrm{SNR}^{-\rho}\right)\right)^i} \\ &\quad \times \left(1 - \Psi \mathrm{SNR}^{-\rho} - o\left(\mathrm{SNR}^{-\rho}\right)\right)^N \qquad (58)\end{aligned}$$

where

$$\Psi \triangleq \alpha \cdot \left(\frac{\epsilon}{KS^2}\right)^{(K-1)S-L+1}. \tag{59}$$

Here, (57) follows from Lemma 1 and from choosing ϵ small enough such that $\frac{\epsilon \mathrm{SNR}^{-1}}{KS^2} < 1$ for given SNR, and (58) follows from $\frac{N!}{i!(N-i)!} \leq N^i$.

Now, if $N = \omega\left(\mathrm{SNR}^{\rho}\right)$, $\left(1 - \Psi \mathrm{SNR}^{-\rho} - o\left(\mathrm{SNR}^{-\rho}\right)\right)^N$ decreases exponentially as SNR increases. On the other hand, $\left\{N\left(\Psi \mathrm{SNR}^{-\rho} + o\left(\mathrm{SNR}^{-\rho}\right)\right)\right\}^i$ increases polynomially for any $i > 0$, and thus, the second term of (58) tends to zero as $\mathrm{SNR} \to \infty$. Therefore, the lower bound of $\mathcal{P}_{\mathrm{SVD}}$ given in (55) tends to 1, which proves the theorem together with (50).

APPENDIX IV
PROOF OF THEOREM 3

Following (33) to (35) and (53) to (55) and denoting the scheme indicator by $\tau \in \{\mathrm{AS}, \mathrm{SVD}\}$, $\mathcal{P}_\tau$ with the cell-dependent parameters can be written by

$$\begin{aligned}\mathcal{P}_\tau &\geq \lim_{\mathrm{SNR}\to\infty} \Pr\left\{\sum_{i=1}^{K}\sum_{j=1}^{S_i}\sum_{j'=1}^{S_i} \eta_\tau^{[i,j']} \mathrm{SNR} \leq \epsilon\right\} \qquad (60) \\ &\geq \lim_{\mathrm{SNR}\to\infty} \Pr\left\{\eta_\tau^{[i,j']} \leq \frac{\mathrm{SNR}^{-1}\epsilon}{\sum_{i'=1}^{K} {S_{i'}}^2}, \forall i \in \mathcal{K}, \forall j' \in \mathcal{S}\right\} \qquad (61) \\ &= \lim_{\mathrm{SNR}\to\infty} \prod_{i=1}^{K} \underbrace{\Pr\left\{\eta_\tau^{[i,j']} \leq \frac{\mathrm{SNR}^{-1}\epsilon}{\sum_{i'=1}^{K} {S_{i'}}^2}, \forall j' \in \mathcal{S}\right\}}_{\triangleq \mathcal{P}_\tau^{[i]}}, \qquad (62)\end{aligned}$$

where in (62), $\mathcal{P}_{\tau}^{[i]}$ denote the probability there exist at least S_i users with LIF metrics smaller than $\frac{\mathrm{SNR}^{-1}\epsilon}{\sum_{i'=1}^{K} {S_{i'}}^2}$ at the i-th cell, which is independent from those of the other cells.

i) Antenna selection-based OIA: Since $\left\| {\mathbf{U}_k}^H \mathbf{h}_{k,\hat{l}(i,j)}^{[i,j]} \right\|^2$ is a Chi-square random variable with DoF of $2S_k$, the scheduling metric $\eta_{\mathrm{AS}}^{[i,j]}$ in (14) is a Chi-square random variable with DoF of $2S'$, where $S' = 2\sum_{k\neq i,k=1}^{K} S_k$. The rest of the proof can be done analogously to the proof for Theorem 1 replacing $(K-1)S$ with S'.

ii) SVD-based OIA: Since ${\mathbf{U}_k}^H \mathbf{H}_k^{[i,j]}$ is an $(S_k \times L_i)$ dimensional Gaussian matrix, $\mathbf{G}^{[i,j]}$ defined in (18) is now $(S' \times L_i)$-dimensional. Following the analogous derivation of the proof for Theorem 2 and replacing $(K-1)S$ with S', we can complete the proof.

REFERENCES

[1] H. J. Yang, W.-Y. Shin, B. C. Jung, and A. Paulraj, "Opportunistic interference alignment of MIMO IMAC : Effect of user scaling over degrees-of-freedom," in *Proc. IEEE Int'l Symp. Inf. Theory (ISIT)*, Cambridge, MA, July 2012, pp. 2646–2650.

[2] V. R. Cadambe and S. A. Jafar, "Interference alignment and degrees of freedom of the K-user interference channel," *IEEE Trans. Inf. Theory*, vol. 54, no. 8, pp. 3425–3441, Aug. 2008.

[3] S. A. Jafar and S. Shamai (Shitz), "Dgrees of freedom region of the MIMO X channel," *IEEE Trans. Inf. Theory*, vol. 54, no. 1, pp. 151–170, Jan. 2008.

[4] M. A. Maddah-Ali, A. S. Motahari, and A. K. Khandani, "Communication over MIMO X channels: Interference alignment, decomposition, and performance analysis," *IEEE Trans. Inf. Theory*, vol. 54, no. 8, pp. 3457–3470, Aug. 2008.

[5] K. Gomadam, V. R. Cadambe, and S. A. Jafar, "A distributed numerical approach to interference alignment and applications to wireless interference networks," *IEEE Trans. Inf. Theory*, vol. 57, no. 6, pp. 3309–3322, June 2011.

[6] C. Suh and D. Tse, "Interference alignment for cellular networks," in *Proc. 46th Annual Allerton Conf. Communication, Control, and Computing*, Urbana-Champaign, IL, Sept. 2008, pp. 1037 – 1044.

[7] A. S. Motahari, O. Gharan, M.-A. Maddah-Ali, and A. K. Khandani, "Real interference alignment: exploiting the potential of single antenna systems," *IEEE Trans. Inform. Theory*, submitted for publication, Preprint, [Online]. Available: http://arxiv.org/abs/0908.2282.

[8] T. Gou and S. A. Jafar, "Degrees of freedom of the K user M X N MIMO interference channel," *IEEE Trans. Inf. Theory*, vol. 56, no. 12, pp. 6040–6057, Dec. 2010.

[9] V. R. Cadambe and S. A. Jafar, "Degrees of freedom of wireless X networks," in *Proc. IEEE Int'l Symp. Inf. Theory (ISIT)*, Toronto, Canada, July 2008, pp. 1268–1272.

[10] ——, "Interference alignment and the degrees of freedom of wireless X networks," *IEEE Trans. Inf. Theory*, vol. 55, no. 9, pp. 3893–3908, Sept. 2009.

[11] T. Gou and S. A. Jafar, "Degrees of freedom of the k user MIMO interference channel," in *Proc. Asilomar Conf. Signals, Systems and Computers*, Pacific Grove, CA, Oct. 2008, pp. 126 – 130.

[12] B. Nazer, M. Gastpar, S. A. jafar, and P. Viswanath, "Ergodic interference alignment," in *Proc. IEEE Int'l Symp. Inf. Theory (ISIT)*, Seoul, Korea, June-July 2009, pp. 1769–1773.

[13] B. C. Jung and W.-Y. Shin, "Opportunistic interference alignment for interference-limited cellular TDD uplink," *IEEE Commun. Lett.*, vol. 15, no. 2, pp. 148–150, Feb. 2011.

[14] B. C. Jung, D. Park, and W.-Y. Shin, "A study on the optimal degree-of-freedoms of cellular networks: Opportunistic interference mitigation," in *Proc. Asilomar Conf. Signals, Systems and Computers*, Pacific Grove, CA, 2010, pp. 2067–2071.

[15] S.-H. Hur, B. C. Jung, and B. D. Rao, "Sum rate enhancement by maximizing SGINR in an opportunistic interference alignment," in *Proc. Asilomar Conf. Signals, Systems and Computers*, Pacific Grove, CA, 2011, pp. 354–358.

[16] B. C. Jung, D. Park, and W.-Y. Shin, "Opportunistic interference mitigation achieves optimal degrees-of-freedom in wireless multi-cell uplink networks," *IEEE Trans. Commun.*, vol. 60, no. 7, pp. 1935–1944, Jul. 2012.

[17] H. J. Yang, W.-Y. Shin, B. C. Jung, and A. Paulraj, "A feasibility study on opportunistic interference alignment: Limited feedback and sum-rate enhancement," in *Proc. Asilomar Conf. Signals, Systems and Computers*, Pacific Grove, CA, 2012.

[18] K. Gomadam, V. R. Cadambe, and S. A. Jafar, "Approaching the capacity of wireless networks through distributed interference alignment," in *Proc. IEEE GLOBECOM*, New Orleans, LO, Nov.-Dec. 2008.

[19] C. M. Yetis, T. Gou, S. A. Jafar, and A. H. Kayran, "On feasibility of interference alignment in MIMO interference networks," *IEEE Trans. Inf. Theory*, vol. 58, no. 9, pp. 4771–4782, Sept. 2010.

[20] H. Sung, S.-H. Park, K.-J. Lee, and I. Lee, "Linear precoder designs for k-user interference channels," *IEEE Trans. Wireless Commun.*, vol. 9, no. 1, pp. 291–301, Jan. 2010.

[21] T. Kim, D. J. Love, and B. Clerckx, "On the spatial degrees of freedom of multicell and multiuser MIMO channels," *IEEE Trans. Inform. Theory*, submitted for publication, Preprint, [Online]. Available: http://arxiv.org/abs/1111.3160 2011.

[22] B. Mondal and R. W. Heath, Jr., "Performance analysis of quantized beamforming MIMO systems," *IEEE Trans. Signal Process.*, vol. 54, no. 12, pp. 4753–4766, Dec. 2006.

[23] T. Yoo, N. Jindal, and A. Goldsmith, "Multi-antenna downlink channels with limited feedback and user selection," *IEEE J. Select. Areas Commun.*, vol. 25, no. 7, pp. 1478–1491, Sept. 2007.

[24] J. Thukral and H. Bölcskei, "Interference alignment with limited feedback," in *Proc. IEEE Int'l Symp. Inf. Theory (ISIT)*, Seoul, Korea, July 2009, pp. 1759–1763.

[25] R. T. Krishnamachari and M. K. Varanasi, "Interference alignment under limited feedback for MIMO interference channels," in *Proc. IEEE Int'l Symp. Inf. Theory (ISIT)*, AUstin, TX, June 2010, pp. 619–623.
[26] S. Pereira, A. Paulraj, and G. Papanicolaou, "Opportunistic scheduling for multiantenna cellular: Interference limited regime," in *Proc. Asilomar Conference on Signals, Systems and Computers*, Pacific Grove, CA, Nov. 2007.
[27] L. Dritsoula, Z. Wang, H. R. Sadjadpour, and J. J. Garcia-Luna-Aceves, "Antenna selection for opportunistic interference management in MIMO broadcast channels," in *Proc. IEEE Signal Process. Advances Wireless Commun. (SPAWC)*, Marrakech, Morocco, June 2010.
[28] Z. Wang, M. Ji, H. R. Sadjadpour, and J. J. Garcia-Luna-Aceves, "Interference management: a new paradigm for wireless cellular networks," in *Proc. IEEE Military Commun. Conf. (MILCOM)*, Boston, MA, Oct. 2009.
[29] N. Jindal, "MIMO broadcast channels with finite-rate feedback," *IEEE Trans. Inf. Theory*, vol. 52, no. 11, Nov. 2006.
[30] L. Wang, Q. Li, S. Li, and J. Chen, "A general algorithm for uplink opportunistic interference alignment in cellular network," in *IEEE GLOBECOM Workshops*, Houston, TX, Dec. 2011, pp. 433–440.
[31] J. Tang, A. J. Anandkumar, and S. Lambotharan, "Opportunistic MIMO multi-cell interference alignment techniques," in *Proc. IEEE Int'l Conf. Internet Multimedia Systems Architecture and Application (IMSAA)*, Bangalore, India, Dec. 2011.
[32] E. Chu and A. George, *Inside the FFT Black Box: Serial and Parallel Fast Fourier Transform Algorithms*. CRC Press, 1999.
[33] S. Boyd and L. Vandenberghe, *Convex Optimization*. Cambridge, U.K.: Cambridge Univ. Press, 2004.
[34] J. M. Chambers, "Algorithm 410: Partial sorting," *Communications of the ACM*, vol. 14, no. 5, pp. 357–358, May 1971.
[35] G. H. Golub and C. F. V. Loan, *Matrix Computations*, 3rd ed. Johns Hopkins University Press, 1996.
[36] A. Edelman, "Eigenvalues and condition numbers of random matrices," Ph.D. dissertation, Messachusetts Institute of Technology, 1989.
[37] S. Jin, M. R. McKay, X. Gao, and I. B. Collings, "MIMO multichannel beamforming: SER and outage using new eigenvalue distributions of complex noncentral Wishart matrices," *IEEE Trans. Commun.*, vol. 56, no. 3, pp. 424–434, Mar 2008.

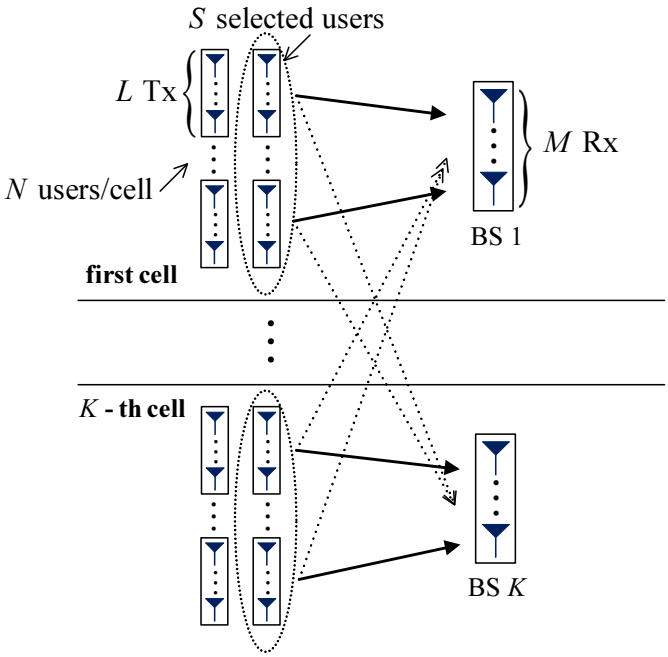


Fig. 1. K-cell MIMO Interfering MAC.

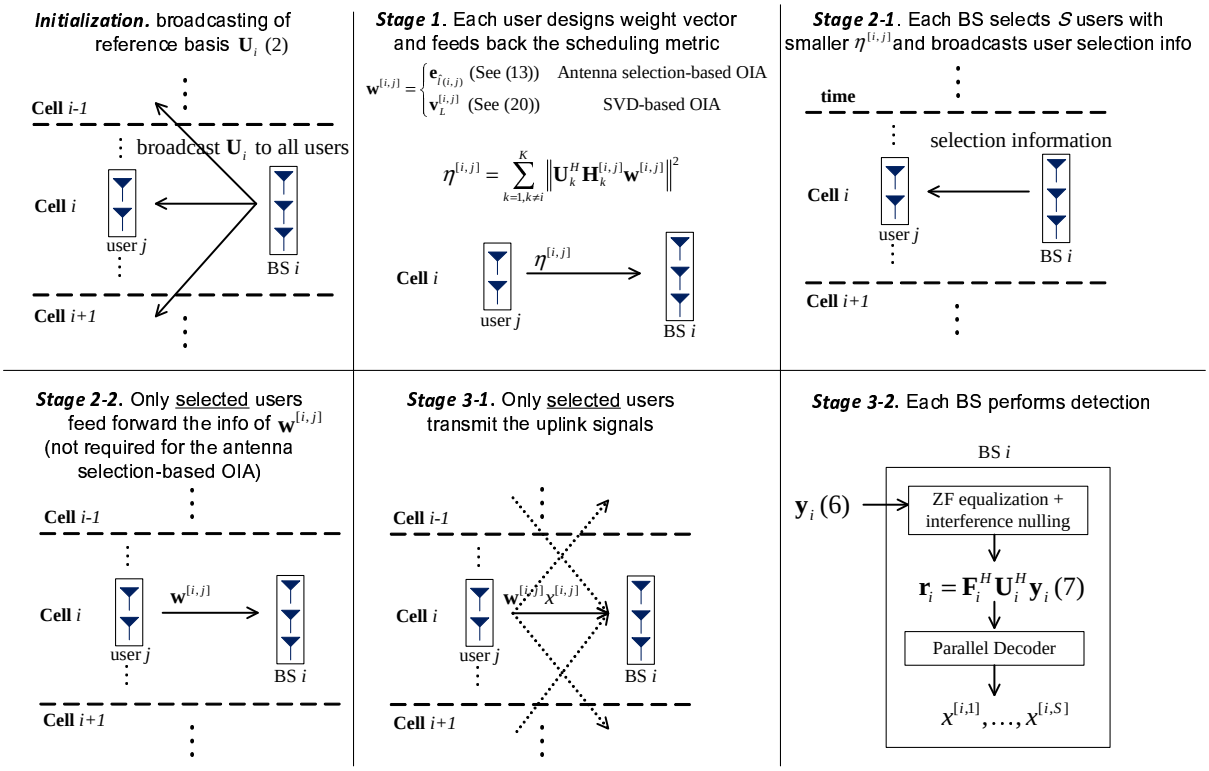


Fig. 2. Overall sequential procedure of the proposed MIMO OIA.

TABLE I

COMPUTATIONAL COMPLEXITY OF THE OIA SCHEMES (FLOPS).

	SIMO OIA [15]	Antenna selection-based OIA	SVD-based OIA
User	$O(KMS)$	$O(KLMS)$	$O(KSL^2 + KLMS)$
BS	$O(N + MS^2)$	$O(N + MS^2)$	$O(N + MLS + MS^2)$

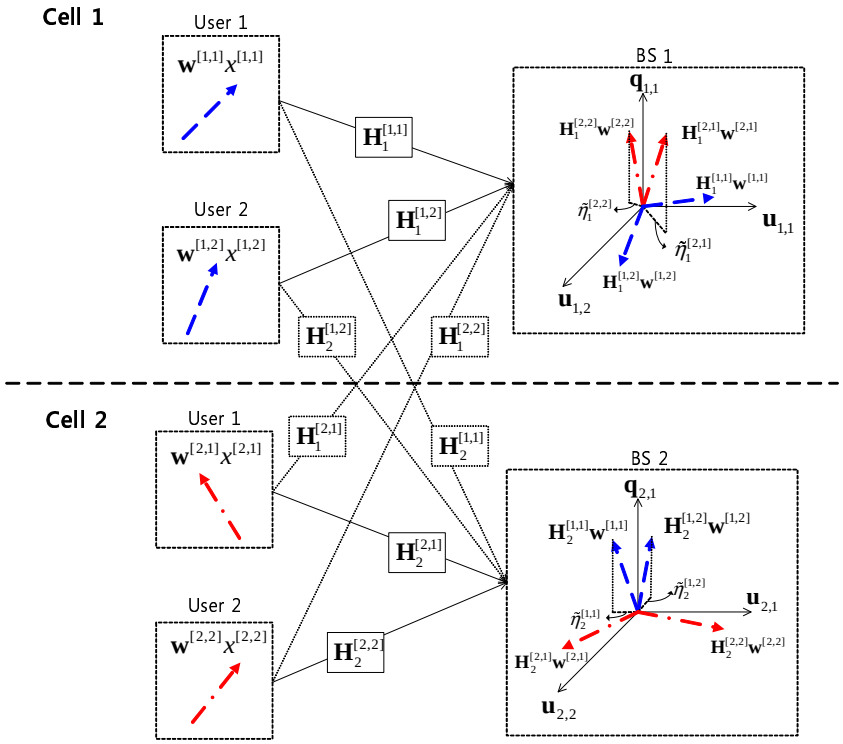


Fig. 3. Proposed MIMO OIA where $K = 2$, $M = 3$, and $S = 2$.

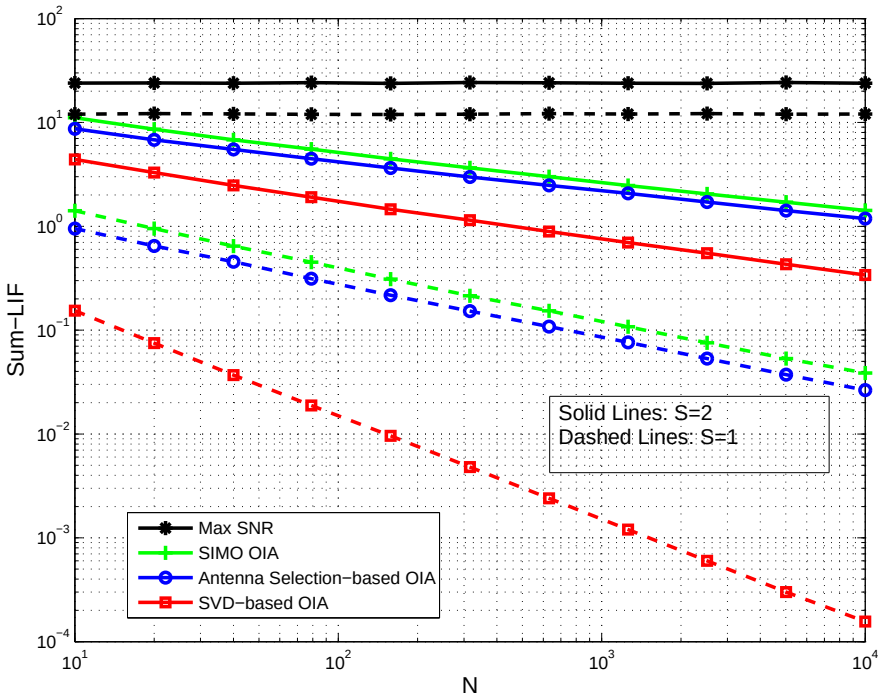


Fig. 4. Sum-LIF versus N for the MIMO IMAC with $K = 3$ and $M = L = 2$.

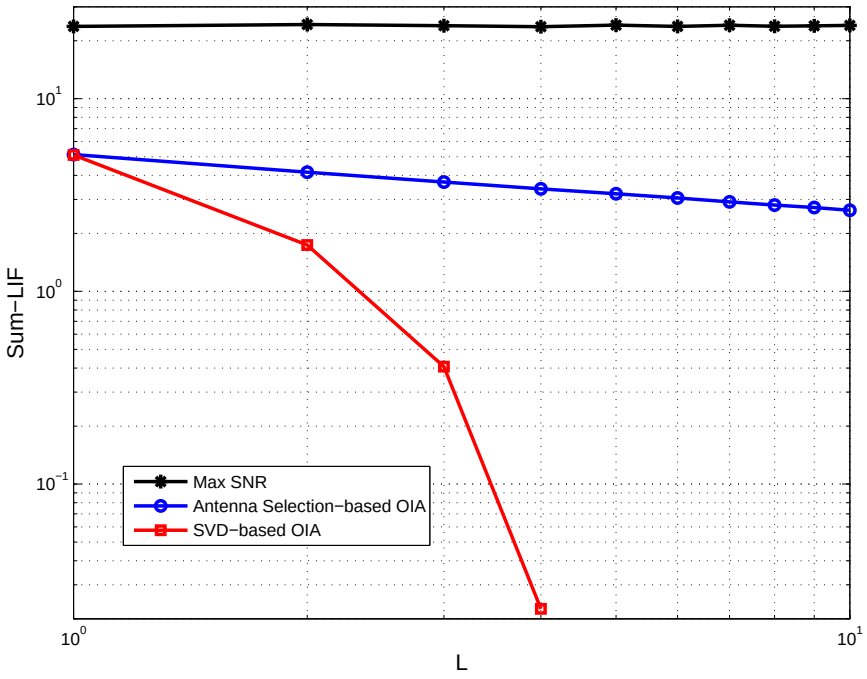
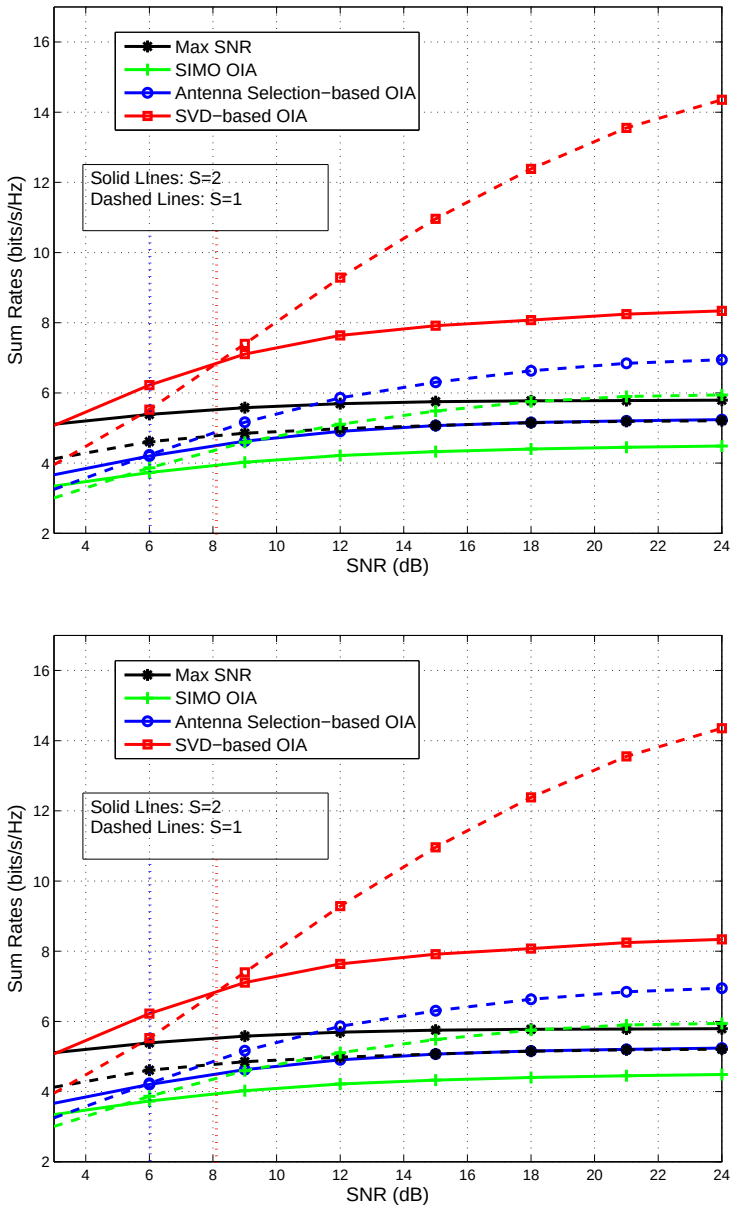


Fig. 5. Sum-LIF versus L for the MIMO IMAC with $K = 3$, $M = 2$, and $N = 100$.



(b)

Fig. 6. Achievable sum-rates versus SNR when $K = 3$, $M = L = 2$, and (a) $N = 20$ and (b) $N = 100$.

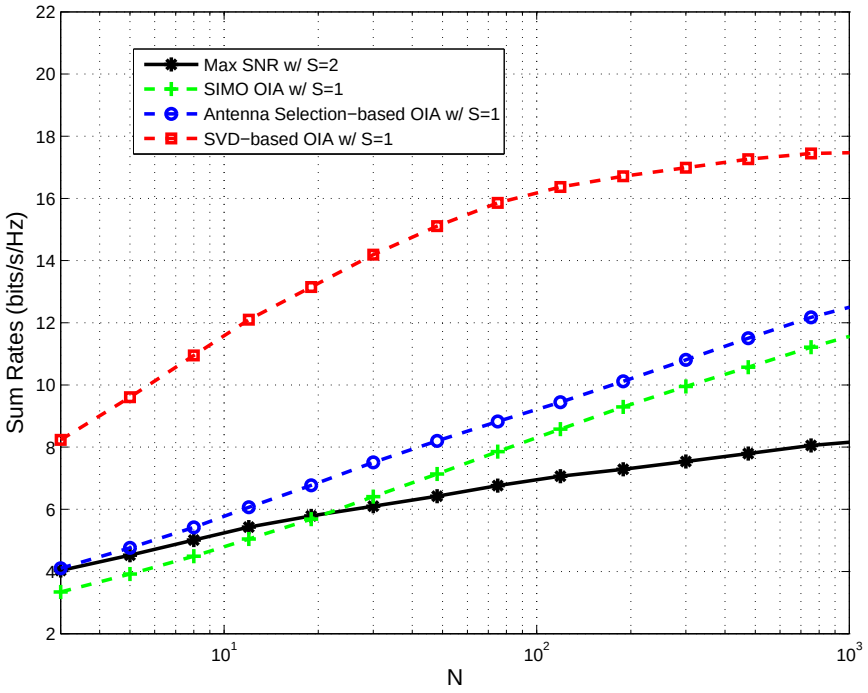


Fig. 7. Achievable sum-rates versus N when $K = 3$, $M = L = 2$, and SNR=20dB.

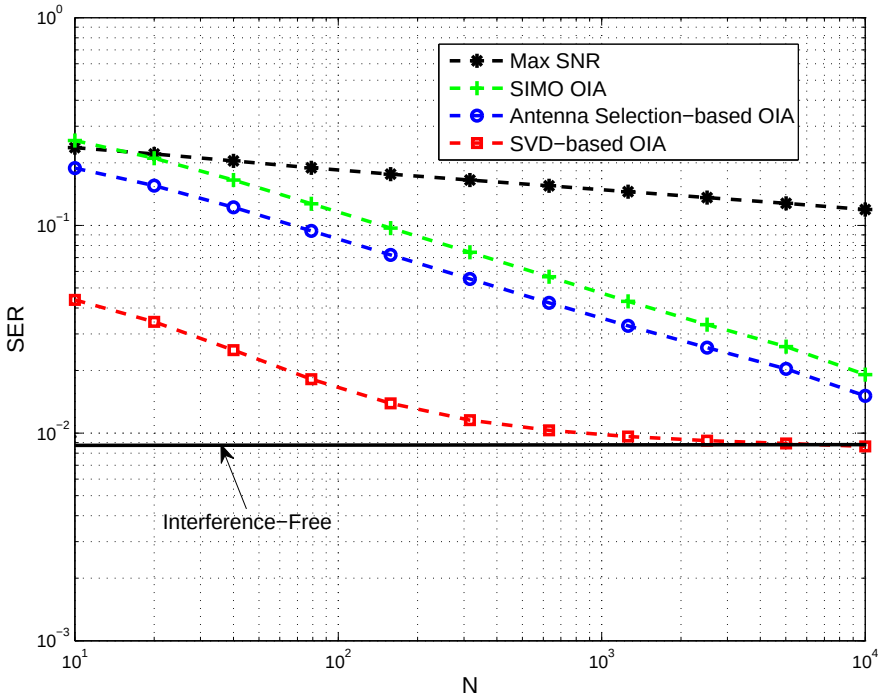


Fig. 8. Average SER versus N with QPSK signaling when $K = 3$, $M = L = 2$, $S = 1$, and SNR=20dB.